

Soret/Dufour Effects on Radiative Free Convection Flow and Mass Transfer over a Sphere with Velocity Slip and Thermal Jump

Shalini JAIN^{1,2,*} and Shweta BOHRA^{1,3}

¹*Department of Mathematics & Statistics, Manipal University Jaipur, Jaipur 303007, India*

²*Department of Mathematics, University of Rajasthan, Jaipur 302004, India*

³*Department of Basic Science, Sangam University, Bhilwara 311001, India*

(*Corresponding author’s e-mail: drshalinijainshah@gmail.com)

Received: 28 January 2017, Revised: 7 August 2018, Accepted: 25 September 2018

Abstract

In this paper, a steady free convective heat and mass transfer boundary layer flow of an electrically conducting viscous fluid from a sphere in a porous medium with thermal radiation is studied. Soret and Dufour effects, velocity slip, and thermal slip are considered at the boundary. The governing PDE is transformed into non-linear ODE using suitable similarity transformations and solved numerically using bvp4c solver of MATLAB. The effect of Schmidt number (Sc), concentration to thermal buoyancy ratio parameter (N_b), Dufour number (Du), Soret number (Sr), radiation parameter (N), permeability parameter (K), dimensionless velocity slip parameter (γ), and dimensionless thermal jump parameter (ϕ) on velocity, temperature and concentration fields, skin friction, and heat and mass transfer rates are analyzed and presented through graphs and tables.

Keywords: Natural convective flow, Soret and Dufour effect, velocity and thermal slip

Nomenclature

a	radius of sphere	C_∞	ambient concentration
r	radial distance from symmetrical axis to surface of the sphere	N	radiation parameter
C_p	specific heat at constant pressure	Pr	Prandtl number
k_0	permeability of porous medium	Re	Reynolds number
K	non-dimensional permeability parameter	Gr	Grashof number
q_r	radiative heat flux	Sc	Schmidt number
σ_1	Stephan-Boltzmann constant	N_b	buoyancy ratio parameter
k_1	mass absorption coefficient	Sr	Soret number
k	thermal conductivity	Du	Dufour number
D_m	mass diffusivity	C_f	skin friction coefficient
K_T	thermal diffusion ratio	Nu	Nussel number
C_s	concentration susceptibility	Sh	Sherwood number
N_0	velocity slip factor	α	thermal diffusivity
K_0	thermal jump factor	β	thermal expansion
u	velocity component in the x direction	β^*	concentration expansion
v	velocity component in the y direction	μ	viscosity

q_w	rate of heat transfer	ν	kinematic viscosity
m_w	rate of mass transfer	Ψ	Stream function
T	temperature	σ	electrical conductivity
T_w	temperature of surface of the sphere	τ_w	shear stress
T_∞	ambient temperature	γ	velocity slip parameter
T_m	mean fluid temperature	ϕ	thermal jump parameter
C	concentration	η	dimensionless radial coordinate
C_w	concentration of surface of the sphere	ξ	dimensionless tangential coordinate

Introduction

In nuclear progress and in much chemical engineering, boundary layer flow over or on various shapes, such as cylinders, cones, ellipses, and spherical geometries, are encountered and has been a very popular research topic for many years. Several studies have considered heat and/or mass transfer from curved bodies like cylinders, cones, spheres, etc. Bachok and Ishak [1] studied heat transfer effect over a stretching cylinder by considering prescribed surface heat flux. Chamkha and Quadri [2] investigated heat and mass transfer from a permeable cylinder embedded in a porous medium with a magnetic field. Researchers such as Chauhan *et al.* [3], Manjunatha *et al.* [4], and Jain and Parmar [5] have considered the flow over a stretching cylinder in porous medium with MHD. Ramanaiah and Malarvizhi [6] have investigated flow over a wedge and a cone under mixed thermal boundary conditions. Sohoulil *et al.* [7] applied HAM method to obtain the solution of flow of Darcian fluid with natural convection through a vertical full cone.

Similarly, a study of convective boundary layer flow over or on a sphere is a huge area of interest nowadays. Earlier, Chiang *et al.* [8] considered surface heat flux and prescribed surface temperature to investigate flow over a sphere. Later on, Chen and Mucoglu [9] gave their contributions in the study of mixed, forced, and free convection about a sphere. Analysis of suction/injection effect on natural convection fluid flow from a sphere was performed by Huang and Chen [10]. Study of natural convection boundary layer flow by considering 2 different boundary conditions, namely constant heat flux (CHF) and constant wall temperature (CWT), has been done by Nazar *et al.* [11,12]. They took 2 types of fluids, 1) Viscous, and 2) Micropolar fluid, in his investigation. Molla *et al.* [13] have analyzed Conjugate effect of thermal and concentration with chemical reactions on free convection flow from an isothermal sphere. Cheng [14] studied the same above study in a micropolar fluid with constant wall temperature and concentration.

In nuclear power plants, thermal energy stores and gas turbines require high operating temperatures on boundary layer flow, with quite significant radiation effect. Further, some researchers have been studying natural convection flow from a sphere with magnetic and radiation effects. Amongst them, Akhtar and Alim [15] have analyzed free convective flow around a sphere in the presence of radiation. They considered constant surface heat flux and solved numerically the governing problem. Later on, Molla *et al.* [16] and Alkasasbeh *et al.* [17] studied the influence of radiation on natural convective laminar flow from an isothermal sphere. They considered convective boundary conditions.

In all the above studies Soret and Dufour effects were assumed to be negligible, due to these small order of magnitude, but Soret and Dufour effects are often applied in the study of power industry problems like nuclear waste disposal, energy transfer in a wet cooling tower, geothermal energy process, and chemical process engineering for separating intermediate molecular weight gases. These are caused when heat and mass transfer occur simultaneously in a moving fluid. Chapman and Cowling [18] have presented several cases when the Dufour effect cannot be neglected. Earlier, from the kinetic theory of gases, Eckert and Drake [19] developed the Soret and Dufour effects on heat and mass transfer, and detailed study has been done by Hirshfelder *et al.* [20] who derived the necessary formulae to calculate the thermal-diffusion coefficient and the thermal diffusion factor for monatomic gases or for polyatomic

gas mixtures. Later on, Dursunkaya and Worek [21] investigated Soret and Dufour effects on both unsteady and steady natural convection from vertical surfaces. Abreu *et al.* [22] addressed Soret and Dufour effects on both free and forced convection boundary layer flows. Further work has been done on Soret and Dufour work with different kind of geometries [23-30]. The study of Soret and Dufour effects on natural convective flow from a permeable sphere immersed in a high porosity medium was examined by Kabeir *et al.* [31]. They applied chemical reaction in the study of mass transfer. Gaffar *et al.* [32], Rao *et al.* [33], and Beg *et al.* [34] have given their contributions to the study of fluid flow, heat-mass transfer for non-Newtonian fluids, such as viscoelastic Jeffrey fluid, tangent Hyperbolic fluid, and micropolar fluid, respectively, from a permeable isothermal sphere with the combined effects of Soret and Dufour. Recently, Chamkha *et al.* [35] presented a numerical solution for the study of convective flow over a sphere in the presence of chemical reaction and Soret-Dufour effect.

In recent years, the slip-flow regime has been widely studied, and researchers have been concentrating on the analysis of micro-scale in micro-electro-mechanical systems (MEMS) associated with the embodiment of velocity slip and temperature jump. Rashidi and Freidoonimehr [36] and Jain and Bohra [37] investigated effects of velocity slip and temperature jump on the flow over a porous rotating disk. The combined effects of temperature and velocity jump on the heat transfer, fluid flow, and entropy generation over a single rotating disk have been examined by Arikoglu *et al.* [38]. Chauhan and Kumar [39] investigated radiation effects on unsteady flow through a porous medium channel with velocity and temperature slip boundary conditions.

The main goal of the present study is to investigate radiation and Soret/Dufour effects in the steady natural convective flow over a sphere in porous medium, which has not yet been done from a literature survey. Gaffar *et al.* [40] applied thermal and hydrodynamic slip conditions for the non-linear steady boundary layer flow and heat transfer of an incompressible Tangent Hyperbolic non-Newtonian fluid from an isothermal sphere. The novelty of the present problem is to investigate flow, heat, and mass transfer with velocity slip and thermal jump with combined effects of Soret/Dufour on flow, heat, and mass transfer; these have been obtained and are depicted graphically.

Mathematical formulation

Consider a steady, 2 dimensional laminar free convective flow over a sphere of radius 'a', heated to temperature T_w and concentration C_w . The sphere is surrounded by a viscous incompressible fluid having ambient temperature T_∞ and far field concentration C_∞ . The system is considered as a fully saturated porous medium in the presence of thermal radiation effect, as shown in **Figure 1**. The x and y coordinates are measured along the surface of the sphere from the lowest point and normal along the surface of the sphere, respectively. $r = a \sin\left(\frac{x}{a}\right)$ is the radial distance from the symmetrical axis to the surface of the sphere.

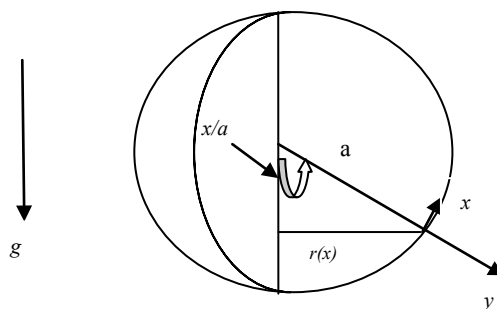


Figure 1 Schematic diagram of problem.

Under the Boussinesq and boundary layer approximations, governing equations can be written in 2 dimensional Cartesian coordinates (x, y) , given by [8,9,13,41,42];

$$\frac{\partial}{\partial x}(ru) + \frac{\partial}{\partial y}(rv) = 0, \tag{1}$$

$$u \frac{\partial u}{\partial x} + v \frac{\partial u}{\partial y} = \nu \frac{\partial^2 u}{\partial y^2} + g\beta(T - T_\infty) \sin\left(\frac{x}{a}\right) + g\beta^*(C - C_\infty) \sin\left(\frac{x}{a}\right) - \frac{\nu u}{k_0}, \tag{2}$$

$$u \frac{\partial T}{\partial x} + v \frac{\partial T}{\partial y} = \alpha \frac{\partial^2 T}{\partial y^2} + \frac{D_m K_T}{C_s C_p} \frac{\partial^2 C}{\partial y^2} - \frac{1}{\rho C_p} \frac{\partial q_r}{\partial y}, \tag{3}$$

$$u \frac{\partial C}{\partial x} + v \frac{\partial C}{\partial y} = D_m \frac{\partial^2 C}{\partial y^2} + \frac{D_m K_T}{T_m} \frac{\partial^2 T}{\partial y^2}, \tag{4}$$

where, u, v are the velocity components along the x, y directions, respectively. $\nu = \frac{\mu}{\rho}$ is kinematic viscosity, ρ is density, T and C are the temperature and concentration, g is the acceleration due to gravity, β and β^* are the coefficients thermal expansion and concentration expansion, respectively. $\alpha = \frac{k}{\rho C_p}$ is the thermal diffusivity, k is thermal conductivity, D_m is the mass diffusivity, T_m is the mean fluid temperature, K_T is thermal diffusion ratio, C_s is the concentration susceptibility, C_p is the specific heat capacity, k_0 is the permeability coefficient, σ_0 is the electric conductivity, and q_r is the radiative heat flux.

The radiative heat flux q_r is simplified by using the Rosseland approximation for radiation;

$$q_r = -\frac{4\sigma_1}{3k_1} \frac{\partial T^4}{\partial y},$$

where σ_1 is the Stefan–Boltzmann constant and k_1 is the mean absorption coefficient. We assume that the temperature differences within the flow are such that the term T^4 may be expressed as a linear function of temperature. This is accomplished by expanding T^4 in a Taylor series about T_∞ and neglecting second and higher order terms; we get;

$$T^4 \cong 4T_\infty^3 T - 3T_\infty^4, \tag{5}$$

$$\frac{\partial q_r}{\partial y} = \frac{\partial}{\partial y} \left(\frac{-4\sigma_1}{3k_1} \frac{\partial T^4}{\partial y} \right) = \frac{\partial}{\partial y} \left(\frac{-4\sigma_1}{3k_1} \frac{\partial (4T_\infty^3 T - 3T_\infty^4)}{\partial y} \right) = \frac{-16\sigma_1 T_\infty^3}{3k_1} \frac{\partial^2 T}{\partial y^2},$$

subject to the boundary conditions as [40];

$$\text{at } y = 0, \quad u = N_0 \frac{\partial u}{\partial y}, \quad v = 0, \quad T = T_w + K_0 \frac{\partial T}{\partial y}, \quad C = C_w,$$

$$\text{at } y \rightarrow \infty, \quad u \rightarrow 0, \quad T \rightarrow T_\infty, \quad C \rightarrow C_\infty. \tag{6}$$

where N_0 is the velocity slip factor, K_0 is the thermal jump factor.

To convert the above governing equations with boundary conditions in non-dimensional form, we introduce the following similarity transformations as [34,40];

$$\xi = \frac{x}{a}, \quad \eta = \frac{y}{a} Gr^{1/4}, \quad \psi = r v \xi f(\xi, \eta) Gr^{1/4}, \quad Gr = \frac{g \beta (T_w - T_\infty) a^3}{\nu^2},$$

$$\theta(\xi, \eta) = \frac{T - T_\infty}{T_w - T_\infty}, \quad \phi(\xi, \eta) = \frac{C - C_\infty}{C_w - C_\infty}, \quad (7)$$

where Gr is thermal Grashof number. This indicates the relative importance of the buoyancy term, compared to the viscous term in natural convection. A large value of Gr , therefore, indicates small viscous effects in momentum equation, similar to the physical significance of Re in a forced flow. We take $Gr > 0$, corresponding to the cooling problem. The transition flow occurs in the range $10^8 < Gr < 10^9$ for natural convection; at lower Grashof number, the boundary layer is laminar.

The stream function ψ is defined by $u = \frac{1}{r} \frac{\partial \psi}{\partial y}$ and $v = -\frac{1}{r} \frac{\partial \psi}{\partial x}$.

The boundary layer Eqs. (1) - (4) with boundary condition (6) are reduced into non-dimensional form by using Eq. (7); applying (5), we get;

$$f''' + (1 + \xi \cot \xi) f f'' - f'^2 + \frac{\sin \xi}{\xi} (\theta + N_b \phi) - \frac{1}{K} f' = \xi \left(f' \frac{\partial f'}{\partial \xi} - f'' \frac{\partial f}{\partial \xi} \right), \quad (8)$$

$$\frac{1}{Pr} \left(1 + \frac{4}{3} N \right) \theta'' + (1 + \xi \cot \xi) f \theta' + Du \phi'' = \xi \left(f' \frac{\partial \theta}{\partial \xi} - \frac{\partial f}{\partial \xi} \theta' \right), \quad (9)$$

$$\frac{1}{Sc} \phi'' + (1 + \xi \cot \xi) f \phi' + Sr \theta'' = \xi \left(f' \frac{\partial \phi}{\partial \xi} - \frac{\partial f}{\partial \xi} \phi' \right), \quad (10)$$

Under the boundary conditions;

$$\text{at } \eta = 0 \quad f(0) = 0, \quad f'(0) = \gamma f''(0), \quad \theta(0) = 1 + \varphi \theta'(0), \quad \phi(0) = 1,$$

$$\text{at } \eta \rightarrow \infty \quad f' \rightarrow 0, \quad \theta \rightarrow 0, \quad \phi \rightarrow 0, \quad (11)$$

where the primes denote the differentiation with respect to η the dimensionless radial coordinate, and ξ is the dimensionless tangential coordinate.

$Pr = \frac{\nu}{\alpha}$, is Prandtl number, representing the ratio between momentum and thermal diffusion. The value of Pr varies as a function of fluid and temperature; for 20 °C, it is 0.71 for air, and 7.0 for water.

$Sc = \frac{\nu}{D_m}$, is Schmidt number. Sc represents the ratio of the momentum to the mass diffusivity. For the present study, the value of Schmidt number is taken as ($Sc = 0.22, 0.66, 0.94, 1, 2, 2.62$). This represents the diffusion of hydrogen, oxygen, carbon dioxide, methanol, ethyl benzene and propyl benzene, respectively, in air.

$N_b = \frac{\beta^* (C_w - C_\infty)}{\beta(T_w - T_\infty)}$, is concentration to thermal buoyancy ratio parameter. $N_b=1$ shows the thermal

and species buoyancy forces are of the same order of magnitude and assist each other.

$Du = \frac{D_m K_T (C_w - C_\infty)}{\nu C_s C_p (T_w - T_\infty)}$, $Sr = \frac{D_m K_T (T_w - T_\infty)}{\nu T_m (C_w - C_\infty)}$, are Dufour and Soret number, respectively.

Dufour number signifies the contribution of the concentration gradients to the thermal energy flux in the flow, and Soret number represents the effect of the temperature gradient on mass (species) diffusion. The Soret effect has been utilized for isotope separation in a mixture between gases with very light molecular weight (He, H₂) and of medium molecular weight (N₂, air).

$N = \frac{4\sigma_1 T_\infty^3}{k_1 k}$, $K = \frac{k_0 \sqrt{Gr}}{a^2}$, $\gamma = \frac{N_0 Gr^{1/4}}{a}$ and $\varphi = \frac{K_0 Gr^{1/4}}{a}$ are radiation parameter, permeability

parameter, dimensionless velocity slip parameter, and dimensionless thermal jump parameter, respectively.

For the present study, physical quantities are:

Local Skin friction coefficient C_f (normalized surface shear stress function);

$$C_f = \frac{\tau_w}{\rho U_\infty^2},$$

For natural convection $\rho U_\infty^2 \approx ag\Delta\rho$, $U_\infty^2 = \frac{ag\Delta\rho}{\rho} = \frac{a^3 g (\Delta\rho/\rho)}{\nu^2} \left(\frac{\nu^2}{a^2}\right) = Gr \left(\frac{\nu^2}{a^2}\right)$

$$C_f = \frac{\tau_w a^2}{\mu \nu^2 Gr}, \text{ Here } \tau_w = \mu \left(\frac{\partial u}{\partial y}\right)_{y=0} = \frac{\mu \nu Gr^{3/4}}{a^2} \xi f''(\xi, 0),$$

Therefore, $Gr^{1/4} C_f = \xi f''(\xi, 0)$.

Local Nusselt number Nu (dimensionless surface heat transfer rate);

$$Nu = \frac{aq_w}{k(T_w - T_\infty)},$$

Here, $q_w = \left[-k \left(\frac{\partial T}{\partial y}\right) + q_r\right]_{y=0} = \frac{k(T_w - T_\infty) Gr^{1/4}}{a} \left(1 + \frac{4N}{3}\right) [-\theta'(\xi, 0)]$

Therefore, $Gr^{-1/4} Nu = -\left(1 + \frac{4N}{3}\right) \theta'(\xi, 0)$.

Local Sherwood number Sh (dimensionless surface mass transfer rate);

$$Sh = \frac{am_w}{D_m (C_w - C_\infty)},$$

Here, $m_w = -D_m \left(\frac{\partial C}{\partial y}\right)_{y=0} = \frac{D_m (C_w - C_\infty) Gr^{1/4}}{a} [-\phi'(\xi, 0)]$

Therefore, $Gr^{-1/4} Sh = -\phi'(\xi, 0)$.

When the location $\xi \sim 0$, near the lower stagnation point of the sphere, is considered, Eqs. (8) - (10) reduce to the ordinary differential equations;

$$f''' + ff'' - f'^2 + (\theta + N_b\phi) - \left(M + \frac{1}{K}\right)f' = 0, \tag{12}$$

$$\frac{1}{Pr} \left(1 + \frac{4}{3}N\right)\theta'' + f\theta' + Du\phi'' = 0, \tag{13}$$

$$\frac{1}{Sc}\phi'' + f\phi' + Sr\theta'' = 0. \tag{14}$$

Numerical method

The governing system is highly non-linear, consisting of coupled ordinary differential equations that are quite difficult to solve analytically. Moreover, the presence of slip terms in the boundary conditions make the system more complicated. To overcome this deficiency, the system of non-linear ordinary differential Eqs. (8) - (10) with the boundary conditions (11) are solved by using *bvp4c* with MATLAB package for various values of parameters, offered by Kierzenka and Shampine [43]. Many engineering problems have been successfully solved by this method. Many researchers, such as [44-46], have presented the comparative study of their results, solved analytically or numerically by shooting technique with *bvp4c* solver with MATLAB. They found that results are in good agreement. The algorithm of this method is followed by;

Step 1. Convert Eqs. (8) - (10) into a system of first order ODEs.

$$f' = p, \tag{15}$$

$$p' = q, \tag{16}$$

$$\theta' = w, \tag{17}$$

$$\phi' = z, \tag{18}$$

$$q' = p^2 - (1 + \xi \cot \xi)fq - \frac{\sin \xi}{\xi}(\theta + N_b\phi) + \frac{1}{K}p + \xi \left(p \frac{\partial p}{\partial \xi} - q \frac{\partial f}{\partial \xi} \right), \tag{19}$$

$$\frac{1}{Pr} \left(1 + \frac{4}{3}N\right)w' = \xi \left(p \frac{\partial \theta}{\partial \xi} - \frac{\partial f}{\partial \xi} w \right) - (1 + \xi \cot \xi)fw - Duz', \tag{20}$$

$$\frac{1}{Sc}\phi'' = \xi \left(p \frac{\partial \phi}{\partial \xi} - \frac{\partial f}{\partial \xi} z \right) - (1 + \xi \cot \xi) fz - Srw', \tag{21}$$

Under the boundary conditions;

$$\text{at } \eta = 0 \quad f(0) = 0, \quad p(0) = \gamma q(0), \quad \theta(0) = 1 + \phi w(0), \quad \phi(0) = 1,$$

$$\text{at } \eta \rightarrow \infty \quad p \rightarrow 0, \quad \theta \rightarrow 0, \quad \phi \rightarrow 0, \tag{22}$$

Step 2. The MATLAB built-in *bvpinit* is used for the initial mesh and initial guess in BVP, consisting of Eqs. (8) - (10). The general form of *bvpinit* is written in MATLAB as;

$$sol = (\text{initial mesh}, \text{initial guess}) \tag{23}$$

Step 3. The solution is added in the argument of `bvp4c` as follows;

$$\text{solution} = \text{bvp4c}(@\text{bvp}, @\text{bc}, \text{sol}) \tag{24}$$

Step 4. The final form of the solution obtained with `bvp4c` in Eq. (24) is in the structure class of MATLAB. The grid points in the η - direction. For details about `bvp4c`, consult reference [47].

Result and discussion

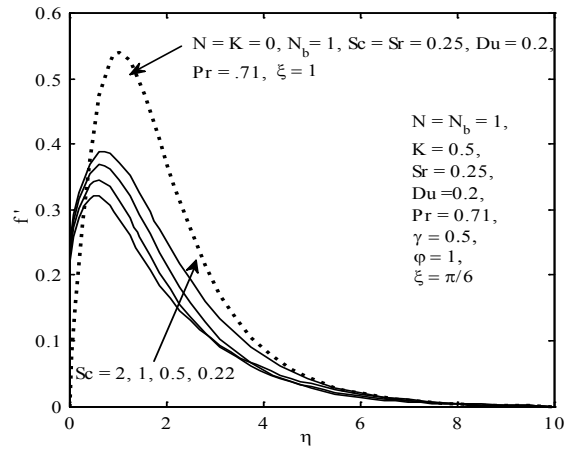
The influence of embedded parameters such as Schmidt number (Sc), concentration to thermal buoyancy ratio parameter (N_b), Dufour number (Du), Soret number (Sr), radiation parameter (N), permeability parameter (K), dimensionless velocity slip parameter (γ), and dimensionless thermal jump parameter (φ) on heat and mass transfer characteristics, with respect to velocity, temperature and concentration profiles, are presented graphically with the help of **Figures 2 - 11**, while the skin friction coefficient (C_f), Nusselt number (Nu) and Sherwood number (Sh) are shown in tabular form as **Table 2**.

From **Figure 2**, we observed that the results obtained are in excellent correlation with the previous study [34]. In **Table 1**, comparison is made for Nusselt number (heat transfer rate) in the absence of permeability, radiation, and Soret and Dufour effects for fixed value of Pr with Nazar *et al.* [11] and Beg *et al.* [34] in no slip condition, and the results are found to be in good agreement.

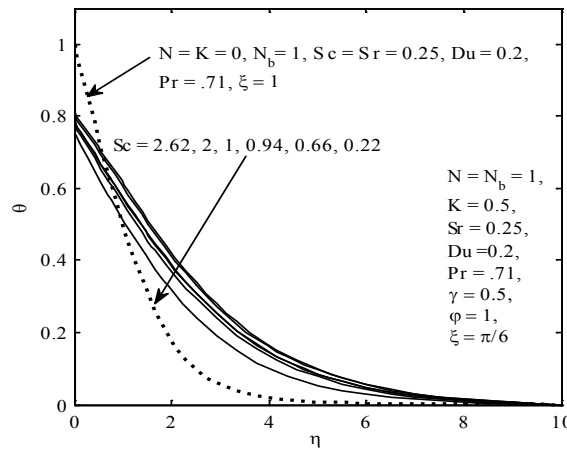
Table 1 Comparison between results of present study with results reported by Nazar *et al.* [11], Bég *et al.* [34], for rate of heat transfer $-\theta'(\xi, 0)$ for $Pr = 0.71$, $Sr = Du = N_b = N = K = \gamma = \varphi = 0$ for Newtonian fluid.

	ξ									
	0^0	10^0	20^0	30^0	40^0	50^0	60^0	70^0	80^0	90^0
Nazar <i>et al.</i> (2002)	0.4576	0.4565	0.4533	0.4580	0.4405	0.4308	0.4189	0.4046	0.3879	0.3684
Beg <i>et al.</i> (2011)	0.4576	0.4565	0.4533	0.4579	0.4405	0.4308	0.4189	0.4046	0.3879	0.3684
Present	0.45916	0.45789	0.45406	0.44757	0.43827	0.42592	0.41008	0.39008	0.36471	0.33159

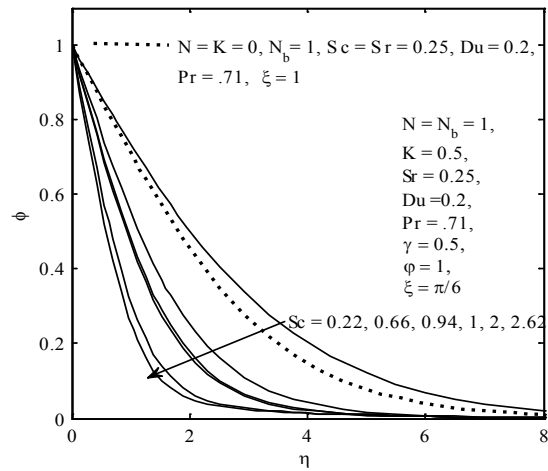
Figures 2(a) - 2(c) shows the effect of Schmidt number Sc on velocity, temperature, and concentration profile. Our numerical calculation is executed for $Pr = 0.71$. The value of Pr is different from Schmidt number, which implies that the thermal and mass diffusion regions are of different extents. The Sc quantifies the relative effectiveness of momentum and mass transport by diffusion in the hydrodynamic (velocity) and concentration (species) boundary layers. It can be seen in **Figures 2(a)** and **2(c)** that velocity and concentration profile decreases when value of Sc number increases; this causes the concentration buoyancy effects to decrease a yielding eradication in fluid velocity, while temperature profile increases with a rise in Sc , as shown in **Figure 2(b)**, because buoyancy-assisted flow is present to boost the temperature.



(a)

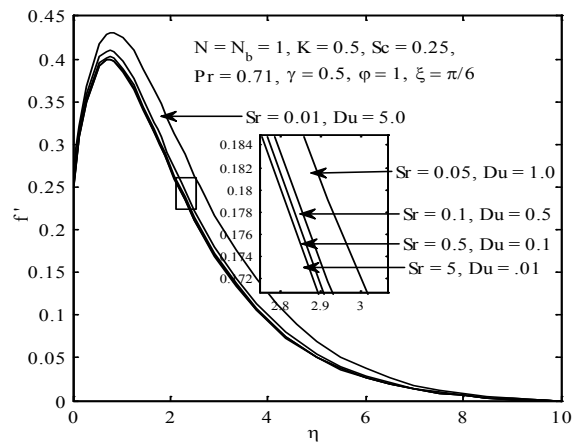


(b)

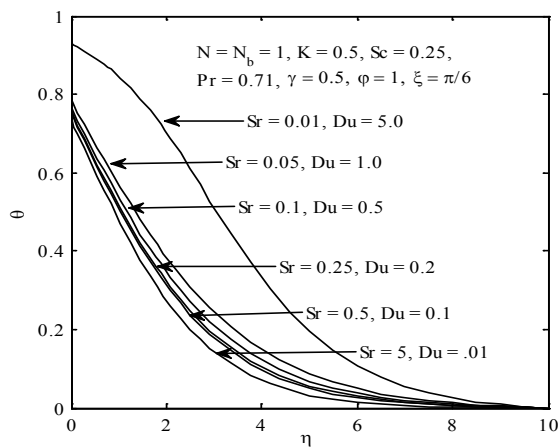


(c)

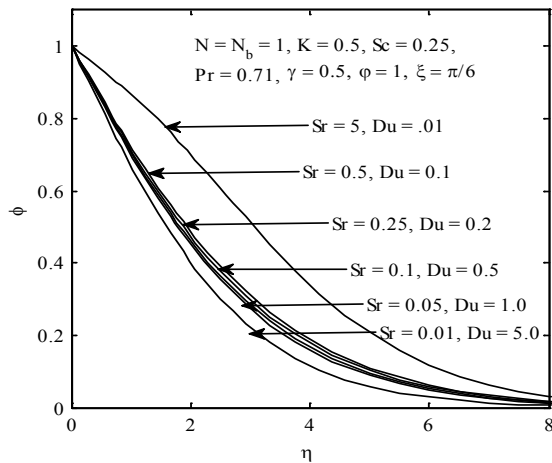
Figure 2 Effect of Sc on (a) velocity profile, (b) temperature profile, (c) concentration profile.



(a)

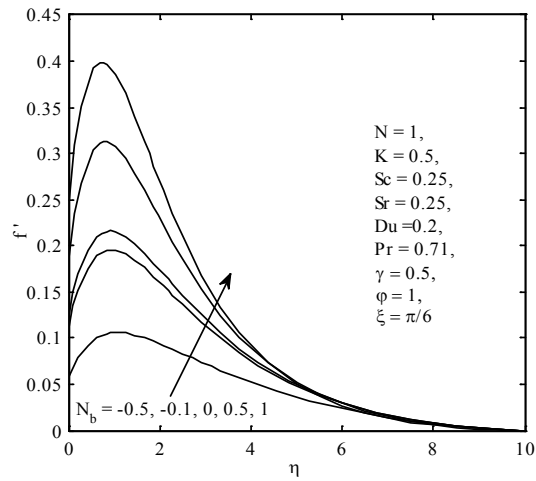


(b)

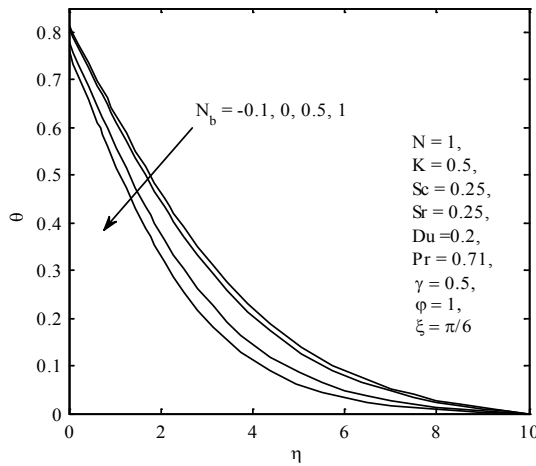


(c)

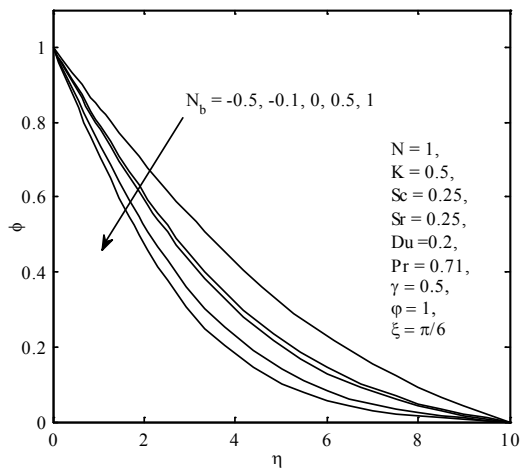
Figure 3 Effect of Sr - Du on (a) velocity profile, (b) temperature profile, (c) concentration profile.



(a)



(b)



(c)

Figure 4 Effect of N_b on the (a) velocity profile, (b) temperature profile, (c) concentration profile.

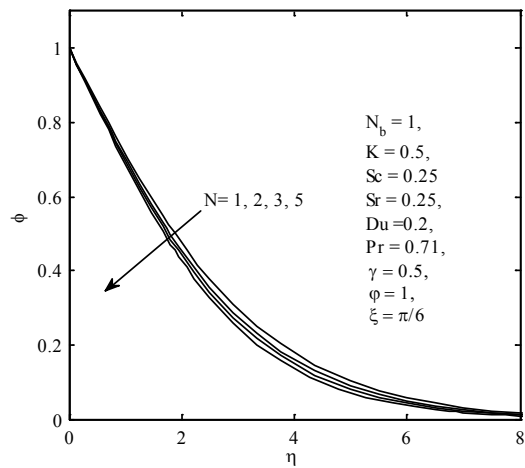
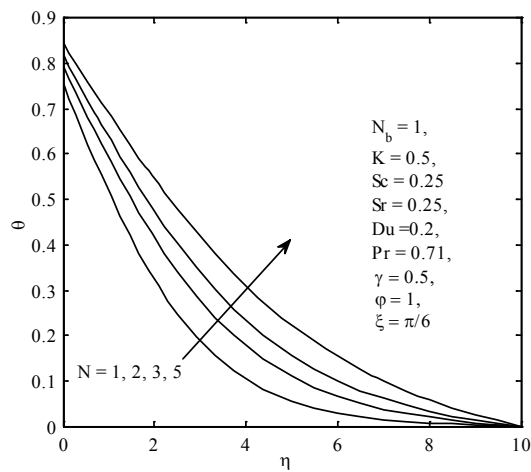
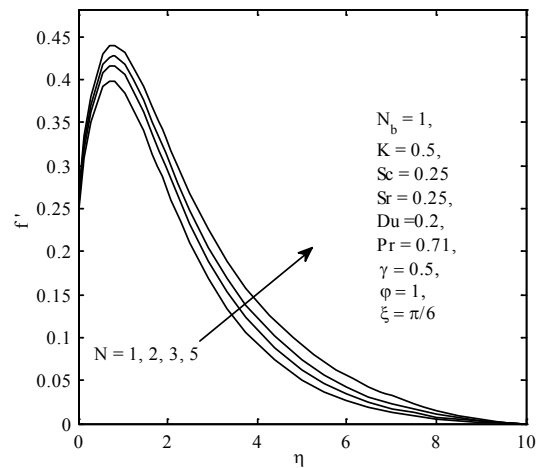


Figure 5 Effect of N on (a) velocity profile, (b) temperature profile, (c) concentration profile.

Figures 3(a) - 3(c) illustrates the combined effect of Soret and Dufour number on velocity, temperature, and concentration distribution. Sr represents the effect of temperature gradients on mass (species) diffusion, whereas Dufour shows the effects of concentration gradient on thermal energy flux. We vary values of Sr and Du in such a way that the product of Sr and Du must stay constant. **Figure 3(a)** depicts that velocity distribution reduces with the combined effect of increasing value of Sr and decreasing value of Du . From **Figure 3(b)**, it can be observed that a decrease in Du (simultaneously increase in Sr) decreases temperature. This is due to the reason that decreasing Du reduces the effect of concentration gradients on the temperature, while decreasing Du enhances the contribution of temperature gradients on concentration profile, which is evidenced by enhanced mass diffusion in the domain. Therefore, concentration boundary layer regime is increased as Du is decreased from 5.0 to 0.01 (and Sr simultaneously increased from 0.01 to 5.0), which is shown in **Figure 3(c)**.

The effect of buoyancy ratio parameter N_b on velocity, temperature, and concentration profile is depicted in **Figures 4(a) - 4(c)**, respectively. **Figure 4(a)** describes that fluid flow is evidently accelerated due to increasing effect of buoyancy ratio parameter, i.e., buoyancy force. The increasing value of N_b shows that flow around the sphere is caused by both temperature and concentration gradients. Therefore, velocity profile increased whereas, from **Figures 4(b) - 4(c)**, we can see that temperature and concentration distribution are reduced when value of N_b increases. Hence, thickness of thermal and concentration boundary layer is reduced, with the effect that surface of sphere is cooled and mass diffusion significantly prevented.

Figure 5 depicts the influence of thermal radiation parameter N on the velocity, temperature, and concentration profiles, It is observed that the N increases thermal radiation of fluid, and thermal energy in boundary layer increases. As a result, both momentum and thermal boundary layer thickness are enhanced with an increment of radiation parameter N , while there is decrement in concentration value with increasing value of N .

Table 2 Variation of $f''(\xi, 0)$, $-\theta'(\xi, 0)$, and $-\phi'(\xi, 0)$ for different values of N , Du , Sr , K , γ , φ , and ξ when $Pr = 0.71$, $Sc = 0.25$, $N_b = 1$.

N	Du	Sr	K	γ	φ	$\xi = 0^\circ$			$\xi = 30^\circ$			$\xi = 60^\circ$		
						$r'(\xi,0)$	$-\theta'(\xi,0)$	$-\phi'(\xi,0)$	$r'(\xi,0)$	$-\theta'(\xi,0)$	$-\phi'(\xi,0)$	$r'(\xi,0)$	$-\theta'(\xi,0)$	$-\phi'(\xi,0)$
1	0.2	0.25	0.5	0.5	1	0.51498	0.25135	0.30144	0.49918	0.24483	0.29106	0.45290	0.22340	0.25840
2						0.53334	0.21110	0.31495	0.51651	0.20554	0.30396	0.46711	0.18755	0.26922
3						0.54450	0.18702	0.32358	0.52696	0.18220	0.31211	0.47540	0.16683	0.27583
1	0.2	0.25	0.5	0.5	1	0.51498	0.25135	0.30144	0.49918	0.24483	0.29106	0.45290	0.22340	0.25840
		0.5				0.51953	0.24132	0.30474	0.50346	0.23510	0.29420	0.45634	0.21470	0.26099
		1.0				0.52726	0.22424	0.31018	0.51072	0.21853	0.29936	0.46219	0.19986	0.26528
1	0.2	0.25	0.5	0.5	1	0.51498	0.25135	0.30144	0.49918	0.24483	0.29106	0.45290	0.22340	0.25840
		0.5				0.51603	0.25239	0.29304	0.50018	0.24584	0.28290	0.45371	0.22432	0.25106
		1.0				0.51818	0.25443	0.27605	0.50220	0.24784	0.26693	0.45535	0.22614	0.23619
1	0.2	0.25	0.1	0.5	1	0.20880	0.16897	0.18471	0.20045	0.16383	0.17848	0.17639	0.14818	0.16016
			0.5			0.51498	0.25135	0.30144	0.49918	0.24483	0.29106	0.45290	0.22340	0.25840
E			1.0			0.63610	0.27343	0.33858	0.61960	0.26717	0.32785	0.57107	0.24635	0.29378
1	0.2	0.25	0.5	0		0.95835	0.23360	0.27541	0.92552	0.22782	0.26657	0.83049	0.20880	0.23861
				0.5		0.51498	0.25135	0.30144	0.49918	0.24483	0.29106	0.45290	0.22340	0.25840

N	Du	Sr	K	γ	ϕ	$\xi = 0^0$			$\xi = 30^0$			$\xi = 60^0$		
						$r'(\xi,0)$	$-\theta'(\xi,0)$	$-\phi'(\xi,0)$	$r'(\xi,0)$	$-\theta'(\xi,0)$	$-\phi'(\xi,0)$	$r'(\xi,0)$	$-\theta'(\xi,0)$	$-\phi'(\xi,0)$
				1		0.34773	0.25718	0.31029	0.33768	0.25048	0.29946	0.30805	0.22838	0.26536
1	0.2	0.25	0.5	0.5	0	0.57494	0.35600	0.31233	0.55598	0.34327	0.30134	0.50034	0.30304	0.26679
				0.5		0.54013	0.29392	0.30617	0.52313	0.28513	0.29554	0.47325	0.25667	0.26211
				1.0		0.51498	0.25135	0.30144	0.49918	0.24483	0.29106	0.45290	0.22340	0.25840

Table 2 presents the influence of various parameters such as radiation parameter N , Dufour number Du , Soret number Sr , permeability parameter K , dimensionless velocity slip parameter γ , and dimensionless thermal jump parameter ϕ on $f'(\xi, 0)$, $-\theta'(\xi, 0)$, and $-\phi'(\xi, 0)$ with constant value of Prandtl number Pr , Schmidt number Sc , and buoyancy ratio parameter N_b . We also considered the variation in tangential coordinate ξ . It has been observed that increasing effect of N , Du , Sr , and K increases the numerical value of $f'(\xi, 0)$, while the reverse result has been obtained when γ and ϕ increases. Numerical value of $-\theta'(\xi, 0)$ reduces when N , Du , and ϕ increases and enhanced with increasing value of Sr , K , and γ . Also, we noticed increment in numerical value of $-\phi'(\xi, 0)$ with increasing N , Du , K , and γ , whereas there is decrement when Sr and ϕ are enhanced.

Figures 6(a) - 6(c) depicts the influence of tangential coordinate ξ on velocity, temperature, and concentration profile. In **Figure 6(a)**, it is noted that velocity profile attains its maximum value at $\xi = 0$, that is, at the lower stagnation point. The transverse coordinate clearly exerts a significant influence on momentum development. Also, as the radial distance increases, the flow decelerates. From **Figures 6(b) - 6(c)**, it can be seen that temperature profile and concentration profile are both strongly enhanced throughout the boundary layer as value of ξ increases. For all values of ξ , temperature attains its maximum value at surface and decreases monotonically as we move away from the surface, although the behavior at the upper stagnation point ($\xi \sim \pi$) is not computed.

Figures 7 and **8** represent the influence of velocity slip and temperature jump on velocity, temperature, and concentration profile. In **Figure 7(a)**, it can be observed that velocity decreases when temperature jump effect increases but, after a saturating point, it increases. Peak velocity attains at no thermal jump ($\phi = 0$). On the value of thermal jump ($St = 3$), maximum deceleration occurs in flow. Temperature profile is also reduced with increasing thermal jump, as shown in **Figure 7(b)**, because heat generation rate is reduced with increasing effect of temperature slip parameter. The maximum effect of thermal jump is shown at the wall of the sphere, which smoothly converges to the vanishing value. Concentration profile is increased when temperature jump increases, but the increment is not very significant, as shown in **Figure 7(c)**. From **Figure 8(a)**, we can see that fluid flow velocity is enhanced near the wall and, after a point, it shows the reverse effect, while temperature and concentration fall down in **Figures 8(b) - 8(c)**. Similar results have been found with the results of Gaffar *et al.* [40].

The influence of permeability parameter on velocity, temperature, and concentration distribution has been plotted in **Figures 9(a) - 9(c)**. It can be noticed that velocity increases with the increasing porosity in domain, while temperature and concentration decrease with the increasing value of K due to decreasing Darcy's resistance force.

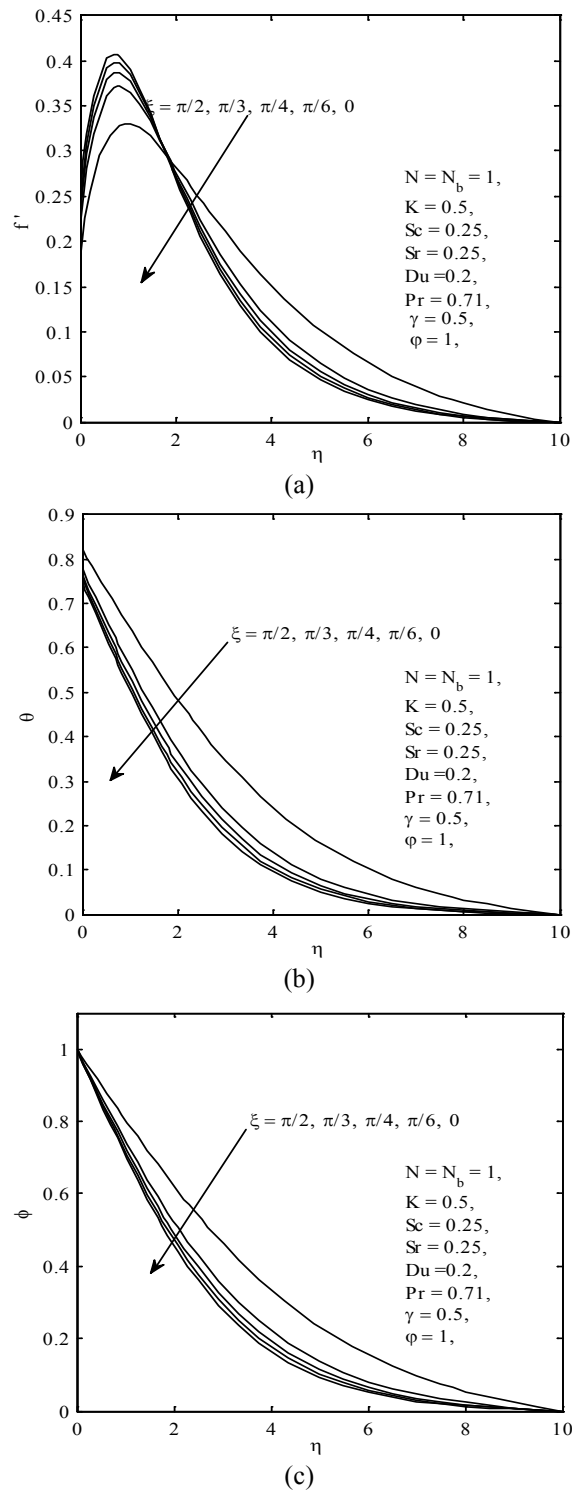


Figure 6 Effect of ξ on (a) velocity profile, (b) temperature profile, (c) concentration profile.

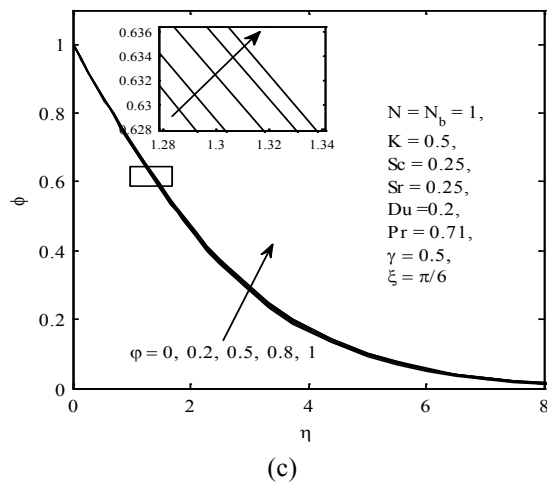
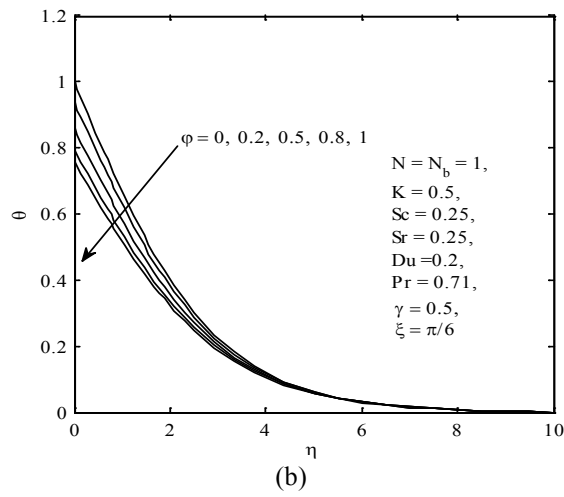
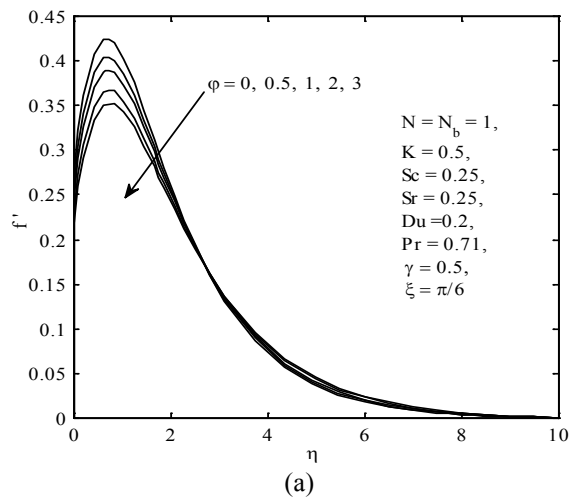


Figure 7 Effect of ϕ on (a) velocity profile, (b) temperature profile, (c) concentration profile.

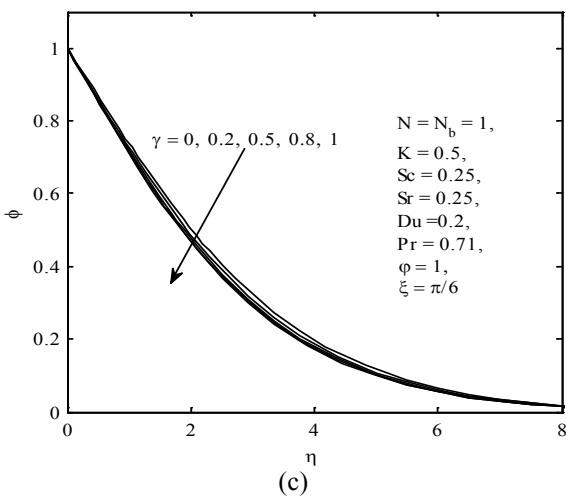
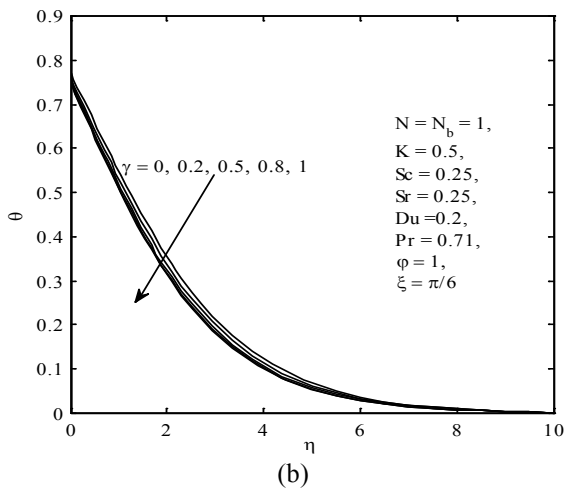
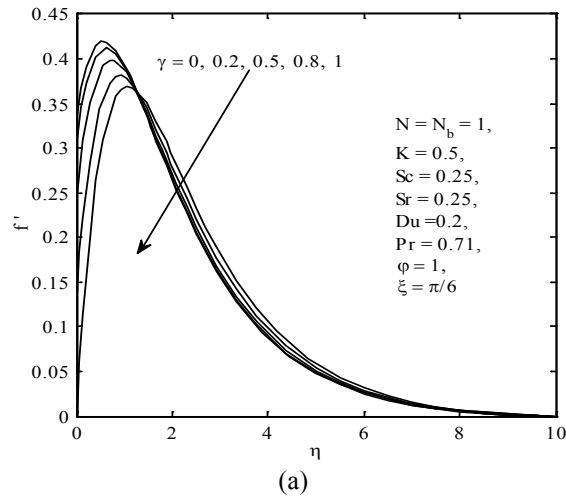


Figure 8 Effect of γ on (a) velocity profile, (b) temperature profile, (c) concentration profile.

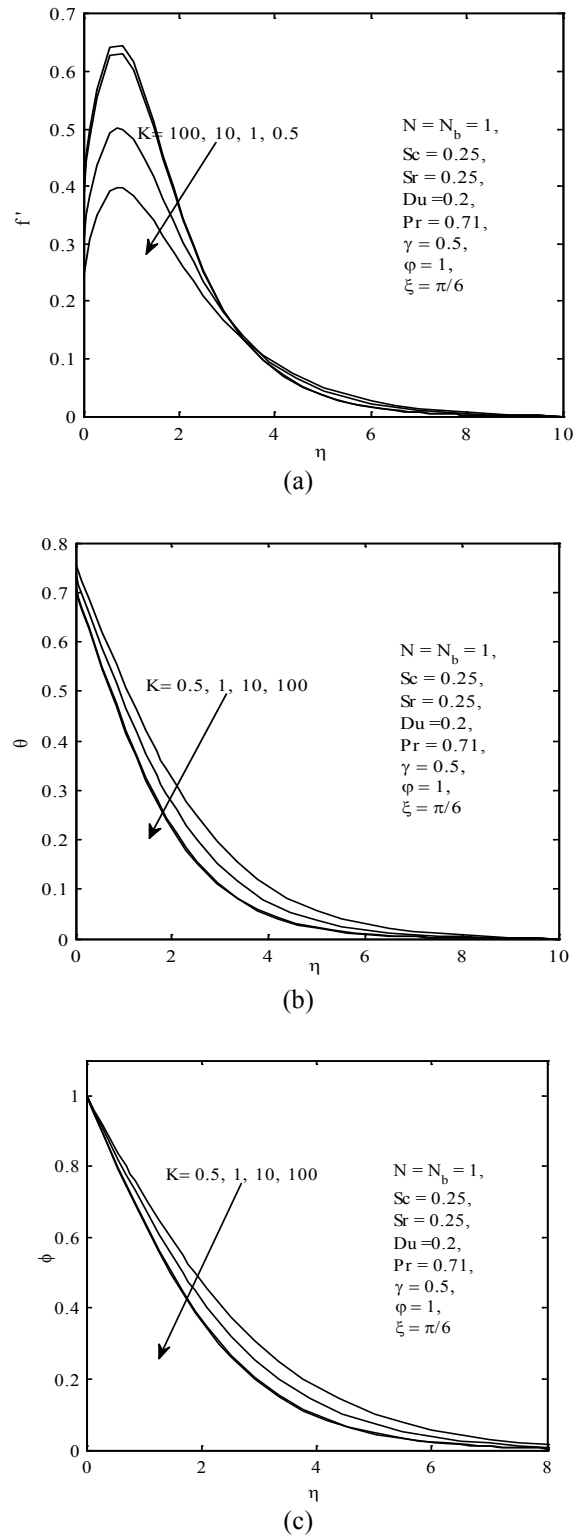


Figure 9 Effect of K on (a) velocity profile, (b) temperature profile, (c) concentration profile.

Conclusions

In this present problem, we studied the 2-dimensional steady laminar free convective boundary layer flow from a sphere. We considered Soret and Dufour effect on fluid flow, heat, and mass transfer. By using bvp4c solver in MATLAB, we obtained the numerical solution for the present investigation. The following conclusions may be drawn:

- Increasing value of Sr (simultaneously decreasing value of Du) increases surface heat transfer rates (Nusselt numbers) but decreases surface mass transfer rates (Sherwood numbers).
- The increasing effect of N_b as Buoyancy-assisted flow accelerates the linear flow field, while decelerating the temperature and mass concentration field.
- The velocity and temperature profiles are enhanced with an increment of radiation, while the reverse effect is shown for concentration.
- When effect of velocity slip is increased, the velocity increases near the wall, whereas an increasing effect of thermal jump reduces velocity. Also, thickness of thermal boundary layer reduces with the increasing effect of velocity slip and temperature jump.

References

- [1] N Bachok and A Ishak. Flow and heat transfer over a stretching cylinder with prescribed surface heat flux. *Malays. J. Math. Sci.* 2010; **4**, 159-69.
- [2] AJ Chamkha and MMA Quadri. Heat and mass transfer from a permeable cylinder in a porous medium with magnetic field and heat generation/absorption effects. *Numer. Heat Trans. Part A* 2001; **40**, 387-401.
- [3] DS Chauhan, P Rastogi and R Agrawal. Magnetohydrodynamic slip flow and heat transfer in a porous medium along a stretching cylinder: Homotopy Analysis Method. *Int. J. Comp. Meth.* 2012; **62**, 136-57.
- [4] PT Manjunatha, BJ Gireesha and BC Prasannakumara. Effect of radiation on flow and heat transfer of MHD dusty fluid over a stretching cylinder embedded in a porous medium in presence of heat source. *Int. J. Appl. Comput. Math.* 2017; **3**, 293-310.
- [5] S Jain and A Parmar. Radiation effect on MHD williamson fluid flow over stretching cylinder through porous medium with heat source. *Lect. Notes Mech. Eng.* 2018; **2018**; 61-78.
- [6] G Ramanaiah and G Malarvizhi. Free convection about a wedge and a cone subjected to mixed thermal boundary conditions. *Acta Mech.* 1992; **93**, 119-23.
- [7] AR Sohouli, D Domairry, M Famouri and A Mohsenzadeh. Analytical solution of natural convection of darcian fluid about a vertical full cone embedded in porous media prescribed wall temperature by means of HAM. *Int. Comm. Heat Mass Trans.* 2008; **35**, 1380-4.
- [8] T Chiang, A Ossin and CL Tien. Laminar free convection from a sphere. *ASME J. Heat Trans.* 1964; **86**, 537-42.
- [9] TS Chen and A Mocoglu. Analysis of mixed forced and free convection about a sphere. *Int. J. Heat Mass Trans.* 1977; **20**, 867-75.
- [10] MJ Huang and CK Chen. Laminar free convection from a sphere with blowing and suction. *ASME J. Heat Trans.* 1987; **109**, 529-32.
- [11] R Nazar, N Amin, T Grosan and IM Pop. Free convection boundary layer on an isothermal sphere in a micropolar fluid. *Int. Comm. Heat Mass. Trans.* 2002; **29**, 377-86.
- [12] R Nazar, N Amin, T Grosan and IM Pop. Free convection boundary layer on a sphere with constant surface heat flux in a micropolar fluid. *Int. Comm. Heat Mass. Trans.* 2002; **29**, 1129-38.
- [13] MM Molla, MA Hossain and RSR Gorla. Conjugate effect heat and mass transfer in natural convection flow from an isothermal sphere with chemical reaction. *Int. J. Fluid Mech. Res.* 2004; **31**, 319-33.
- [14] CY Cheng. Natural convection heat and mass transfer from a sphere in micropolar fluids with constant wall temperature and concentration. *Int. Comm. Heat Mass. Trans.* 2008; **35**, 750-5.

- [15] T Akhter and MA Alim. Effects of radiation on natural convection flow around a sphere with uniform surface heat flux. *J. Mech. Eng.* 2008; **39**, 50-6.
- [16] MM Molla, MA Hossain and S Siddiqa. Radiation effect on free convection laminar flow from an isothermal sphere. *Chem. Eng. Comput.* 2011; **198**, 1483-96.
- [17] HT Alkasasbeh, MZ Salleh, RM Tahar, RM Nazar and IM Pop. Effect of radiation and magnetohydrodynamic free convection boundary layer flow on a solid sphere with convective boundary conditions. *Walailak J. Sci. & Tech.* , 2015; **12**, 849-61.
- [18] S Chapman and TG Cowling. *The Mathematical Theory of Non-uniform Gases*. Cambridge University Press, UK, 1952.
- [19] Eckert and Drake. *Analysis of Heat and Mass Transfer*. Taylor & Francis, 1986.
- [20] JO Hirshfelder, CF Curtis and RB Bird. *Molecular Theory of Gases and Liquids*. Wiley, New York, 1954.
- [21] Z Dursunkaya and WM Worek. Diffusion-thermo and thermal-diffusion effects in transient and steady natural convection from vertical surface. *Int. J. Heat Mass Trans.* 1992; **35**, 2060-7.
- [22] CRA Abreu, MF Alfradique and AS Telles. Boundary layer flows with Dufour and Soret effects: I: Forced and natural convection. *Chem. Eng. Sci.* 2006; **61**, 4282-9.
- [23] N Pandya and AK Shukla. Soret-Dufour and radiation effect on unsteady MHD flow over an inclined porous plate embedded in porous medium with viscous dissipation. *Int. J. Adv. Appl. Math. Mech.* 2014; **2**, 107-19.
- [24] OA Bég, TA Bég, AY Bakier and V Prasad. Chemically-reacting mixed convective heat and mass transfer along inclined and vertical plates with Soret and Dufour effects: numerical solutions. *Int. J. Appl. Math. Mech.* 2009; **5**, 39-57.
- [25] R Bhargava, R Sharma and OA Bég. Oscillatory chemically-reacting MHD free convection heat and mass transfer in a porous medium with Soret and Dufour effects: finite element modeling. *Int. J. Appl. Math. Mech.* 2009; **5**, 15-37.
- [26] E Osalusi, J Side and R Harris. Thermal-diffusion and diffusion-thermo effects on combined heat and mass transfer of a steady MHD convective and slip flow due to a rotating disk with viscous dissipation and Ohmic heating. *Int. Comm. Heat Mass Trans.* 2008; **35**, 908-15.
- [27] A Mahdy. Heat transfer and flow of a Casson fluid due to a stretching cylinder with the Dufour effects. *J. Eng. Phy. Thermophys.* 2015; **88**, 928-36.
- [28] CY Cheng. Soret and Dufour effects on natural convection heat and mass transfer from a vertical cone in a porous medium. *Int. Comm. Heat Mass Trans.* 2009; **36**, 1020-4.
- [29] A Mohan and R Ganapathy. Heat transfer and cross-diffusion due to a sphere of constant thermal energy embedded in a porous medium. *Therm. Sci.* 2017; **21**, S503-S513.
- [30] S Jain and R Chaudhary. Soret and Dufour effects on MHD fluid flow due to moving permeable cylinder with radiation. *Global Stoch. Anal.* 2017; **4**, 75-84.
- [31] SMM EL-Kabeir, AJ Chamkha, AM Rashad and HF Al-Mudhaf. Soret and Dufour effects on heat and mass transfer by nondarcy natural convection from a permeable sphere embedded in a high porosity medium with chemically-reactive species. *Int. J. Energ. Tech.* 2010; **2**, 1-10.
- [32] SA Gaffar, V R Prasad, B Vasu, E Keshava, C Reddy and OA Beg. Thermal radiation and heat generation/absorption effects on viscoelastic double-diffusive convection from an isothermal sphere in porous media. *Ain Shams Eng. J.* 2015; **6**, 1009-30.
- [33] AS Rao, L Nagaraja, MS Reddy and MSN Reddy. Steady -state transport phenomena on induced magnetic field modelling for Non-newtonian tangent hyperbolic fluid from an isothermal sphere with Soret and Dufour effects. *Front. Heat Mass Trans.* 2017; **9**, 17.
- [34] OA Bég, VR Prasad, B Vasu, NB Reddy, Q Li and R Bhargava. Free convection heat and mass transfer from an isothermal sphere to a micropolar regime with Soret/Dufour effects. *Int. J. Heat Mass Trans.* 2011; **54**, 9-18.
- [35] AJ Chamkha, AM Aly and ZAS Raizah. Double-Diffusion MHD free convective flow along a sphere in the presence of a homogeneous chemical reaction and Soret and Dufour effects. *Appl. Comput. Math.* 2017; **6**, 34-44.

- [36] MM Rashidi and N Freidoonimehr. Effects of velocity slip and temperature jump on the entropy generation in magnetohydrodynamic flow over a porous rotating disk. *J. Mech. Eng.* 2012; **1**, 4-14.
- [37] S Jain and S Bohra. Radiation effects in flow through porous medium over a rotating disk with variable fluid properties. *Adv. Math. Phys.* 2016; **2016**, 1-12.
- [38] A Arikoglu, G.Komurgoz, I Ozkol and AY Gunes. Combined effects of temperature and velocity jump on the heat transfer, fluid flow, and entropy generation over a single rotating disk. *J. Heat Trans.* 2010; **132**, 111703-10.
- [39] DS Chauhan and V Kumar. Radiation effects on unsteady flow through a porous medium channel with velocity and temperature slip boundary conditions. *Appl. Math. Sci.* 2012; **6**, 1759-69.
- [40] SA Gaffar, VR Prasad, EK Reddy and OA Bég. Free convection flow and heat transfer of non-newtonian tangent hyperbolic fluid from an isothermal sphere with partial slip. *Arab. J. Sci. Eng.* 2014; **39**, 8157-74.
- [41] I Pop and DB Ingham. *Convective Heat Transfers Mathematical and Computational Modelling of Viscous Fluids and Porous Media*. Pergamon, Amsterdam, 2001.
- [42] K Vajravelu and S Mukhopadhyay. *Fluid Flow, Heat and Mass Transfer at Bodies of Different Shapes: Numerical Solutions*. Academic Press, 2015.
- [43] J Kierzenka and LF Shampine. A BVP solver based on residual control and the Matlab PSE. *ACM Trans. Math. Soft.* 2001; **27**, 299-316.
- [44] S Jain and S Bohra. Heat and mass transfer over a three-dimensional inclined non-linear stretching sheet with convective boundary conditions. *Indian J. Pure Appl. Phys.* 2017; **55**, 847-56.
- [45] T Hayat, S Ali, MA Farooq and A Alsaedi. On comparison of series and numerical solutions for flow of eyring-powell fluid with Newtonian heating and internal heat generation/absorption. *PLoS One* 2015; **10**, 1-13.
- [46] ZG Makukula, P Sibanda, SS Motsa and S Shateyi. On new numerical techniques for the MHD flow past a shrinking sheet with heat and mass transfer in the presence of a chemical reaction. *Math. Probl. Eng.* 2011; **2011**, 489217.
- [47] LF Shampine, J Kierzenka and MW Reichelt. *Solving Boundary Value Problems for Ordinary Differential Equations in MATLAB with bvp4c*. Tutorial Notes, 2000.